The Effect of Nanoparticle Addition on SiC and AlN Powder-Polymer Mixtures: Part I. Packing & Flow Behavior

Valmikanathan P. Onbattuvelli, Ravi K. Enneti,[2] Seong-Jin Park,[3] and Sundar V. Atre[1*]

[1]Oregon State University, Corvallis, OR, USA

[2]Global Tungsten Powders, Towanda, PA, USA

[3]Pohang University of Science & Technology, Republic of Korea

*To whom correspondence should be addressed: sundar.atre@oregonstate.edu

Abstract

The development of methods to increase sintered density and improve dimensional tolerances is a crucial issue in powder metallurgy and ceramic processing. Increasing the packing density of starting powders is one effective route to achieve high sintered density and dimensional precision. The current paper presents an in-depth study on the effect of nanoparticle addition on the powder content of SiC and AlN powder-polymer mixtures. In particular, bimodal mixtures of nanoscale and sub-micrometer particles were found to have significantly increased powder volume fraction (solids loading) in the mixtures for injection molding. This observation to increasing packing density by using nanoparticles is surprising and novel since nanoparticles are known to inherently exhibit poor packing behavior. Additionally, for a given volume fraction of powder, the bimodal μ-n suspensions had a lower viscosity at any shear rate compared to the monomodal μ- suspensions. The ability to lower the suspension viscosity by adding nanoparticles to micron-sized particles has important implications for processing of particulate suspensions by powder injection molding (PIM), extrusion, slip casting and tape casting. Samples made from bimodal powders exhibited slower polymer removal during debinding and higher densification with lower shrinkage on sintering compared to the corresponding samples made from monomodal powder mixtures.

Keywords: Nanoparticles; rheology; packing fraction; bimodal mixtures; silicon carbide, aluminum nitride

1. Introduction

Nanoparticles are of tremendous interest since they have the potential to display enhanced sinterability, finer microstructures and improved properties [1]. However, nanoparticles also typically exhibit poor packing behavior. Additionally, the tendency of fine particles to agglomerate in suspension negatively impacts the rheological behavior and homogeneity of nanoparticle suspensions. Higher green density and homogeneity of powder packing in powder-polymer mixtures are important for improving the sintered density, precision, defect control and ensuing properties [2-5]. Thus, there continue to be major challenges in taking advantage of the enhanced sinter densification of fine powders [6-9] while avoiding many processing problems associated with them [10-12]. Prior studies have also examined the merits of using a wide particle size distribution where small particles fit into the interstitial spaces between large particles [13-16]. However, size segregation is possible with such particle distributions, in turn leading to inhomogeneous microstructures [17]. Different bimodal mixture models have been developed and evaluated in the past in order to predict particle-packing behavior [18-21]. However, their applicability to nanoscale particle sizes where agglomeration dominates has not been examined extensively, especially from the perspective of powder processing into net-shaped architectures.

The present study demonstrates a novel application of nanoparticles for improving the particle packing and flow behavior of bimodal powder mixtures. In the current work, bimodal mixtures of microscale (μ) and nanoscale (n) AlN owders were blended with different ratios with a polymer phase. The effect of the nanoparticle content on powder packing was studied and the bimodal μ-n powder mixture providing the maximum powder-binder mixture density was determined. Additionally, a comparative study between monomodal and bimodal powder-binder mixtures was performed to understand the effect of nanoparticle addition on rheological properties. A similar set of experiments was also conducted with μ-n SiC powder mixtures in order to examine the generality of this packing and rheological behavior initially observed in μ-n AlN powder mixtures. These experiments showed a surprising result that nanoparticles with poor packing characteristics significantly improved packing behavior in bimodal powder-polymer

mixtures. The rheological behavior of such mixtures and the implications for processing by powder injection molding (PIM), extrusion, slip casting and tape casting are presented.

2. Experimental Section

The starting powder materials consisting of commercially available AlN, SiC and Y_2O_3 were used as received. Similar to the earlier reports on PIM, a multicomponent polymer system based on paraffin wax, polypropylene was chosen as the binder to facilitate a multi-step debinding process [22, 23]. Torque rheometry on different ratios of particle sizes was performed in the Intelli-Torque Plasticorder (Brabender) with a maximum chamber volume of 46 cc. The monomodal and bimodal powder-polymer mixture formulations thus determined were then scaled-up in production on a 27 mm co-rotating twin-screw extruder (Entek Extruders) with an L/D ratio of 40. The density for all the extruded mixtures was measured with a lab-built Archimedes apparatus. Rheological characteristics of the extruded mixtures were examined on a Goettfert Rheograph 6000 capillary rheometer at different temperatures (140-180°C). A Rabinowitsch correction was applied to the viscosity data. Micrographs of powder samples were taken with a QuantaTM –FEG (FEI) dual beam scanning electron microscope (SEM) coupled with an energy dispersive X-ray spectrometer (EDS).

A homogeneous powder-polymer mixture is required for consistent part fabrication using the PIM process [22, 23]. The maximum volumetric powder-polymer ratio at which the suspension viscosity is still finite and the powder particles are tightly packed and molten polymer fills all the voids between the particles is called the critical solids loading (Φ_C) [23]. Φ_C was measured by torque rheometry with a starting batch of 70 wt% powder content mixed at 160 °C. The polymer mixture was initially added to the chamber and allowed to melt while being mixed at a programmed speed of 50 rpm. The bimodal μ-n powder mixtures were roll-milled for 30 minutes prior to mixing with the polymer mixture. The roll milled powder mixtures were then slowly added and allowed to blend with the polymers until the mixing torque stabilized. Additional doses of premixed powders were incrementally added to raise the solids loading and the torque was again allowed to stabilize. This procedure was repeated until the mixing torque either did not stabilize or rapidly decreased, both indicating an excess amount of powder. A similar procedure was performed for all bimodal μ-n powder ratios and repeated thrice to check for the

reproducibility. A solids loading ($\Phi < \Phi_C$) was scaled up by twin-screw extrusion and pelletized for further characterization. For scale-up, a solids loading less than the critical solids loading was chosen for processing flexibility to minimize the occurrence of large viscosity changes for minor variations in particle content that is typically observed for concentrated suspensions [24].

3. Results and Discussion

Figure 1 represents the mixing torque as a function of time for incremental powder additions for 100% μ-AlN (a) and μ-SiC (b) powders. It can be seen that for any addition, there is an initial increase in mixing torque followed by stabilization to a lower value when the mixture attains a maximum homogeneity level possible at the shear rate. Further, the mixing torque increases with increasing powder content until a critical point following which the mixing torque falls indicating an excess of powder in the mixture.

There is an upper limit to powder content that is possible in a powder-polymer mixture for any particle size distribution. The particle size distribution was varied by adding nanoparticles to the μ-sized powders. The fraction of n-sized particles in the bimodal μ-n powder mixture was plotted against the maximum powder content in the resulting powder-polymer mixtures as shown in the **Figure 2.** Thus, a maximum powder content of 90 wt. % (~ critical solids loading (Φ_c) of 71 vol.%) in the powder-polymer mixture was achieved for the bimodal AlN mixture containing 82 wt.% μ- AlN and 18 wt.% n-AlN (**Figure 2a**). Similarly, a maximum powder content of 87 wt. % (Φ_c - 65 vol.%) in the powder-polymer mixture was achieved with a particular bimodal mixture containing 90 wt.% μ- SiC and 10 wt.% n-SiC (**Figure 2b**). Comparative experiments for monomodal 100 wt.% μ-SiC and μ-AlN systems, resulted in a maximum powder content of only 81 wt. % (53 vol.% - SiC and 54 vol.% - AlN) in the powder-polymer mixture. Further, the monomodal 100 wt. % n-SiC and n-AlN systems showed a maximum powder content below 75 wt. %. Thus, a synergistically improved packing tendency can be observed for the mixtures of microscale and nanoscale powders.

SEM was performed on the monomodal and bimodal samples to examine the increase in the powder content with the nanoparticle addition for AlN and SiC systems (**Figures 3** and **4**). It can be noticed that in the bimodal powder-polymer mixtures (**Figures 3b** and **4b**), the nanoparticles fit into the interstitial spaces between the microparticles for the AlN and SiC systems, respectively.

The mixing torque is plotted as a function of solids loading in **Figures 5a** and **5b** for the monomodal and bimodal AlN and SiC systems. From the figures, it can be noticed that the mixing torque increases as a function of solids loading for all four material systems. In addition, the mixing torque was found to generally decrease by the addition of nanoparticles in both AlN and SiC mixtures, as shown in the **Figure 5a** and **5b** respectively. This behavior can be attributed to a lower suspension viscosity in bimodal mixtures, possibly due to the higher packing capability observed in the bimodal mixtures leading to lesser hydrodynamic friction between the powder and polymer phases. Such observations can be extended to predict and compare the rheological behavior of the monomodal and bimodal mixtures. For example, Suri et al (**Equation 1**) showed that the viscosity of the powder-polymer mixture is dependent to the hydrodynamic stress (σ_H), the torque rheometer's mixing blade gap thickness (H), screw speed (U_0) and geometric factor (S) [15]:

$$\eta_{mixture} = \frac{3}{10}\left(\frac{(1+S)*H}{U_0}\right)*\sigma_H \qquad (1)$$

Additionally, higher mixing torque values were observed for SiC mixtures compared to AlN mixtures at a comparable solids loading. This observation is likely be due to the shape irregularlity in the SiC particles relative to the AlN particles as seen in **Figures 3** and **4**. Further studies on this behavior could provide reason for the fluctuations in the mixing torque values for lower solids loading in the SiC mixtures. From the above findings, formulations with optimal solids loading (Φ) of 58 and 65 vol.% for bimodal AlN and SiC, respectively, were compounded using twin screw extrusion. The conditions used for the scale-up are listed in the **Table 1**. Similarly, powder-polymer mixtures of monomodal μ-sized SiC and AlN powders with Φ of 51 and 52 vol.%, were also compounded for comparison purposes.

Nanoparticles are well known to exhibit poor packing density owing to their tendency to agglomerate. Hence, the current finding of using nanoparticles to increase the solids loading appears to be rather interesting. However, successful processing of these bimodal mixtures (with higher powder content) is contingent upon an in-depth understanding of the rheological behavior of such mixtures. Thus, the apparent viscosity-shear rate curves of the extruded AlN and SiC powder-polymer mixtures were measured at different temperatures, as shown in the **Figures 6**

and **7**, respectively. In addition, the viscosity of the binder mixture (**Figure 8**) was also measured to model the rheological behavior of bimodal suspensions.

Irrespective of the powder composition, the viscosity of all the powder-polymer mixtures decreased with an increase in shear rate, indicating pseudoplastic behavior. This was confirmed by evaluating the slope of such viscosity plots which represent (n-1), where "n" is the power law coefficient. The plots in our current case hold a negative slope with value of (1-n) [25]. **Table 2** lists the "n" values of the powder-polymer mixtures and the binder mixtures. These values also indicate the absence of dilatant behavior, suggesting no powder-binder separation. The reduced "n" values with the addition of nanoparticles indicate a possible increase in the shear- thinning behavior. An elaborate analysis is however required to evaluate the role of nanoparticles addition on such pseudoplastic behavior. The higher coefficient values of monomodal SiC mixture compared to that of AlN mixture necessitates future studies on the effect that particle shape has on the flow behavior. Additionally, the viscosity of all the powder-polymer mixtures tends to decrease with increasing temperature. This may be attributed to powder volume reduction arising from binder expansion and increased disentanglement of the molecular chains under shear during heating [4].

The viscosity of both AlN (**Figure 6b**) and SiC bimodal powder-polymer mixtures (**Figure 7b**) was found to be higher that of the monomodal powder-polymer mixtures (**Figure 6a and 7a**) at any given shear rate - temperature conditions. This could be due to the increased solids loading as well as the presence of nanoparticles in the mixtures. An attempt was made to analytically separate the contributions of reduced particle size from the increased solids loading by computing viscosity values at comparable solids loadings. A number of theoretical as well as empirical equations have been developed to predict the rheological behavior of suspensions with and without using the Φ_c values [26-31]. However, several of these equations are derived for dilute suspensions of spheres in Newtonian liquids. For the current study, it was necessary to consider models that take into account the maximum powder content Φ_c, for predicting the viscosity of concentrated suspensions.

For our current work on powder-polymer mixtures with higher powder content, the *Krieger-Dougherty* model was used [18, 22] as shown in **Equation 2**:

$$\eta_{mixture} = \eta_{binder} * \left[1 - \frac{\phi}{\phi_c}\right]^{-\phi_c[\eta]} \quad (2)$$

Secondly, a simplified version of the above model [32] was used as shown in **Equation 3**:

$$\eta_{mixture} = \frac{\eta_{binder}}{\left[1 - \frac{\phi}{\phi_c}\right]^2} \quad (3)$$

The variants used in the equation have the same physical meaning; η is the viscosity of the binder or mixture depending on the subscript, [η] is the intrinsic viscosity, Φ is the optimal solids loading, Φ_c is the critical solids loading and "m" generally assumes the value of 2 [36]. In our current work, the [η] corresponding to the particular powder mixtures was determined by rewriting **Equations 2** and **4** as,

$$[\eta] = \frac{\left(\ln[\eta_{mixture}] - \ln[\eta_{binder}]\right)}{-\phi_c * \ln\left[1 - \frac{\phi}{\phi_c}\right]} \quad (4)$$

[η] was calculated using **Equation 4** to be 2.57 (±0.22) and 1.94(±0.14) for monomodal SiC and AlN powder-polymer mixtures, respectively. These values however increased to 3.58 (±0.32) and 3.19(±0.26) for bimodal SiC and AlN mixtures, respectively. These results are supported by similar findings by Liu et al in zirconia-wax systems [26] and by Dabak and Yucel in metal/metal-oxide- organic solvent suspensions [36]. The rheological data was also evaluated by the above method to compute Φ_c that showed similar trends to experimentally determined values of Φ_c by torque rheometry

Equations 2 and **3** was used to compute $\eta_{mixture}$ for various volumetric fractions of powder-polymer mixtures with experimental values of Φ_c. The trends using **Equation 3** are shown in **Figure 9** for AlN (a) and SiC (b) powder-polymer mixtures at shear rates of 160 – 800 s^{-1} and for a melt temperature of 160 °C. Irrespective of the models, the bimodal powder-polymer mixtures tend to show more fluidity than the respective monomodal systems. The lower viscosity in bimodal mixtures can be attributed to the effect of better powder packing and reduced critical solids loading. Ferrini et al reported similar trends in the past by comparing the shear viscosity of glass-beads (of various sizes) suspended in mineral oil [35]. The ability to lower the suspension

viscosity by adding nanoparticles to micron-sized particles has important implications for processing of particulate suspensions by powder injection molding (PIM), extrusion, slip casting and tape casting.

In follow-up experiments, the bimodal AlN and SiC systems showed good injection molding characteristics [5]. Further, the bimodal SiC and AlN samples could be debound completely within practical times (< 4 hours). However, the bimodal systems exhibited slower polymer removal during solvent extraction and thermal debinding process compared to samples made from monomodal powder mixtures [37]. The combined effect of increased powder content and reduced average particle size via nanoparticle addition is inferred as the reason for such behavior. Further, a catalytic effect was observed in bimodal systems possibly due to the presence of nanoparticles resulting in a lowering of thermal decomposition temperature of polymers by 50-100^{o}C. Sintering studies showed the formation of liquid phase at 1500°C in the bimodal AlN and SiC samples, a temperature that is at least 100°C lower than typically reported values in the literature. The sintered parts of bimodal AlN and SiC mixtures exhibited comparable sintered density but lower shrinkage (~14%) than the corresponding monomodal mixtures (~20%). The results from the sintering studies are reported elsewhere [38-39]. Further studies are on-going in order to examine microstructure-property relationships in the bimodal systems.

4. Conclusions

The current work successfully demonstrated the feasibility of significantly increasing the powder content in powder-polymer mixtures by nanoparticle addition to submicron-scale particles using torque rheometry and SEM. This novel principle of bimodal μ–n powder mixtures can also be applied to other material systems and applications through the use of the approach reported in this work. Rheological studies indicated that for comparable solids loading, the bimodal mixtures with nanoscale particles have lower viscosity than corresponding monomodal suspensions. Samples made from bimodal powders exhibited slower polymer removal during debinding and higher densification with lower shrinkage on sintering compared to the corresponding samples made from monomodal powder mixtures.

References

1. Atre, S.V.; Valmikanathan, O.P.; Park, S.J.; and German, R.M.; "Sintering of Metal and Ceramic Nanoparticles," in *Applications of Nanomaterials*, Eds. R. Chaugule and S. Watwe, American Scientific Publishers, FL, 2012.
2. V. Vinothini, P. Singh, M. Balasubramanian, *Journal of Materials Science*, 2006, vol.41, pp. 7082-7087.
3. S.B. Reddy, P.P. Singh,N. Raghu,V. Kumar, *Journal of Materials Science*, 2007, vol.37, pp. 929-934.
4. L. Liu, N.H. Loh, B.Y. Tay, S.B. Tor, Y. Murakoshi, R. Maeda, *Materials Characterization*, 2005, vol. 54, pp. 230-238.
5. V.P. Onbattuvelli, S. Vallury, T. McCabe, S-J. Park, S.V. Atre, *PIM International*, 2010, vol. 4(3), pp. 64-70.
6. M. Trunec, K. Maca, *Journal of American Ceramic Society*, 2007, vol. 90(9), pp. 2735–2740
7. M. Trunec, K. Maca, Z. Shen, *Scripta Materialia*, 2008, vol.59, pp. 23-26
8. R.M.German, *Sintering theory and practice*, 1st edition, 1996, John Wiley and Sons, NY
9. M. Bothara, *Sintering of nanocrystalline silicon carbide in plasma pressure compaction system,* PhD Thesis, 2007, Oregon State University
10. W.Wagner, R.S. Averbach, H. Hahn, W.Petry, A. Wiedmann, *Journal of Materials Research*, 1991, vol.6, pp. 2193-2198
11. K. Wetzel, G. Rixecker, G. Kaiser, F. Aldinger, *Advanced Engineering Materials*, 2005, vol.7 (6), pp. 520-524.
12. C.L. Huang, J.J. Wang, C.Y. Huang, *Materials Letters,* 2005, vol.59(28), pp. 3746-3749
13. J. Hashim, L. Looney, M.S.J. Hashmi, *Journal of Materials Processing Technology*, 2002, vol.123, pp. 251-257
14. G. Skandan, *Nanostructured Materials*, 1995, vol.5, pp.111–126
15. P. Suri, S.V. Atre, R.M. German, J.P. DeSouza, *Materials Science and Engineering A*, 2003, vol. 356, pp. 337-344.
16. L. Qiu, X. Li, Y. Peng, W. Ma, G. Qiu, Y. Sun, *Journal of Rare Earths*, 2007, vol.25 (2), pp. 322-326
17. S.M. Olhero, J.M.F. Ferreira, *Powder Technology*, 2004, vol.139, pp. 69-75
18. R.M. German, *Advances in Powder Metallurgy and Particulate Materials*, 1992, vol. 3, pp. 1-15
19. J. Zheng, W.B. Carlson, J.S. Reed, *Journal of the European Ceramic Society*, 1995, vol.15, pp. 479- 483
20. J-L.Shi, J.D. Zhang, *Journal of American Ceramic Society*, 2000, vol.83 (4), pp. 737-742
21. C.L. Martin, D. Bouvard, *International Journal of Mechanical Sciences*, 2004, vol. 46, pp. 907–927
22. G. Aggarwal, S.J. Park, I. Smid, *International Journal of Refractory Metals and Hard Materials,* 2006, vol. 24, 253–262
23. S.J. Park, Y. Wu, D.F. Heaney, X. Zou, G. Gai, R.M. German, *Metallurgical and Materials Transactions A*, 2009, vol. 40 A, pp. 215-222
24. R.M. German, A. Bose, Injection Molding of Metal and Ceramics, 305-337, MPIF Publication, New Jersey, USA, 1997.
25. R. S. Lib, B.R. Patterson, H.A. Heflin, *Progress in Powder Metallurgy*, 1986, vol. 42, pp. 95-104
26. D-M. Liu, W.J. Tseng, *Journal of Materials Science*, 2000, vol. 35, pp. 1009-1016

27. T. Honek, B. Hausnerova, P. Saha, *T. Bata, Polymer Composites*, 2004, vol. 26(1), pp.29-36.
28. C. Atzeni, L. Massidda, U. Sanna, Comparison between rheological models for Portland cement pastes, *Cement and Concrete Research*, 1985, vol. 15(3), pp. 511-519.
29. A. Grants, A. Irbītis, G. Kroņkalns, M.M. Maiorov*, Journal of Magnetism and Magnetic Materials*, 1990, vol. 85(1-3), pp. 129-132.
30. H.J.H. Brouwers, *Physical Review E*, 2010, vol. 81(5), pp. 051402-1-11.
31. D.L. Faulkner, LL.R. Schmidt, *Polymer Science and Engineering*, 1977, vol.17(9), pp. 657-665.
32. P. C. Hiemenz and R. Rjagopalan, "Principles of Colloid and Surface Science," 169, 3rd ed., Mercel Dekker Inc., New York, USA, 1997.
33. R. Lapasin, S.Pricl, *The Canadian Journal of Chemical Engineering*, 1992, vol. 70(1), pp. 20-27.
34. P.S. Leung, E.D. Goddard, *Langmuir*, 1990, vol. 6(1), pp. 3-6.
35. F. Ferrini, D. Ercolani, B. de Cindio, L. Nicodemo, L. Nicolias, S. Ranaudo, *Rheologica Acta*, 1979, vol. 18(2), pp. 289-296.
36. T. Dabak, O. Yucel, *Rheologica Acta*, 1986, vol. 25(5), pp. 527-533.
37. V.P. Onbattuvelli, R.K. Enneti, S.V. Atre, The Effects of Nanoparticle Addition on Binder Removal from Injection Molded Aluminum Nitride, International Journal of Refractory Metals and Hard Materials, 2012 (submitted).
38. V.P. Onbattuvelli, R.K. Enneti, S.V. Atre, The Effects of Nanoparticle Addition on the Densification and Properties of SiC, *Ceramics International*, (accepted).
39. V.P. Onbattuvelli, R.K. Enneti, S.V. Atre, The Effects of Nanoparticle Addition on the Sintering and Properties of Bimodal AlN, *Ceramics International*, (accepted).

List of Figures:

List of Tables

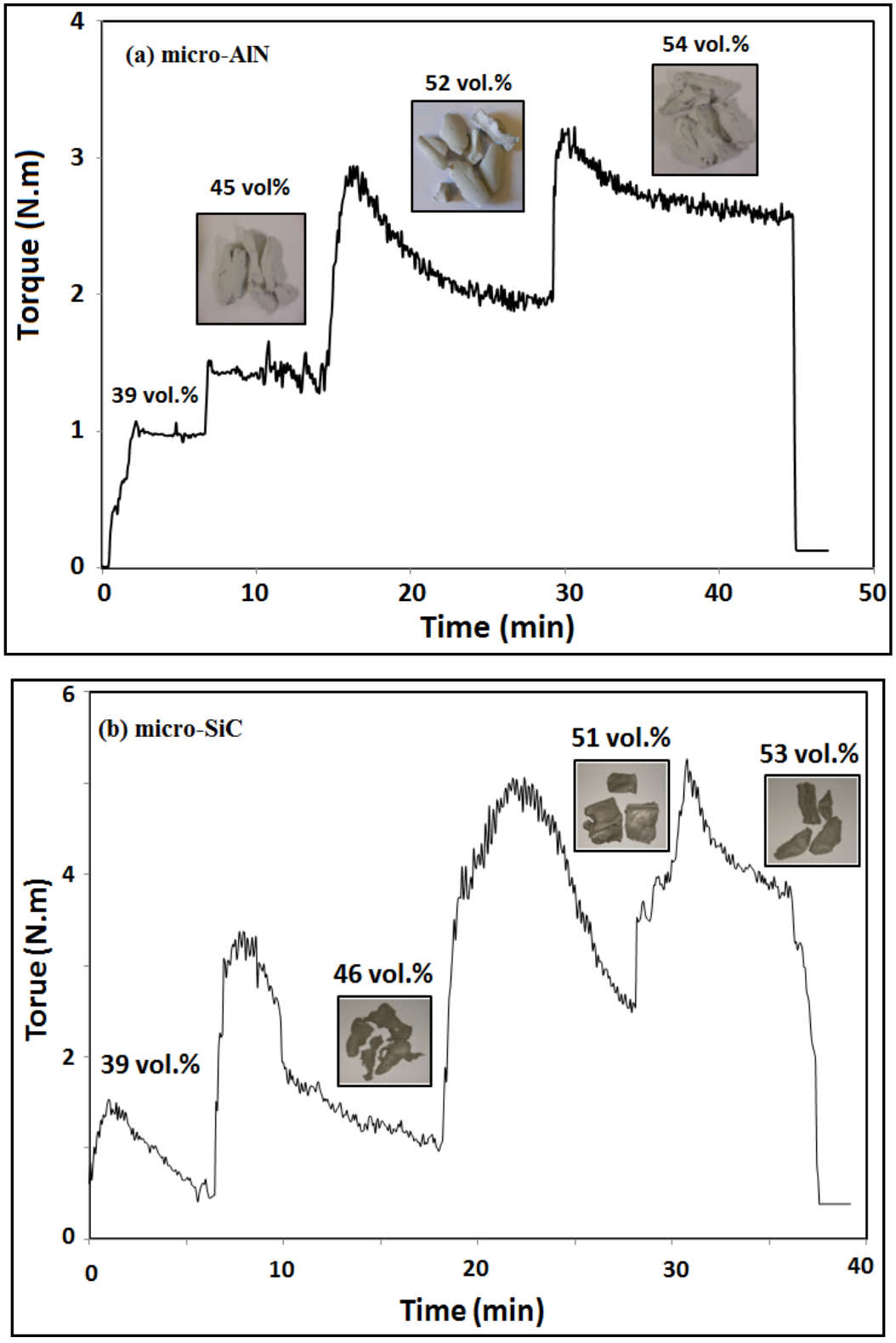

Figure 1: Torque rheometry plot for 100% µ-AlN (a) and µ-SiC (b) with the insets showing the resulting mixtures

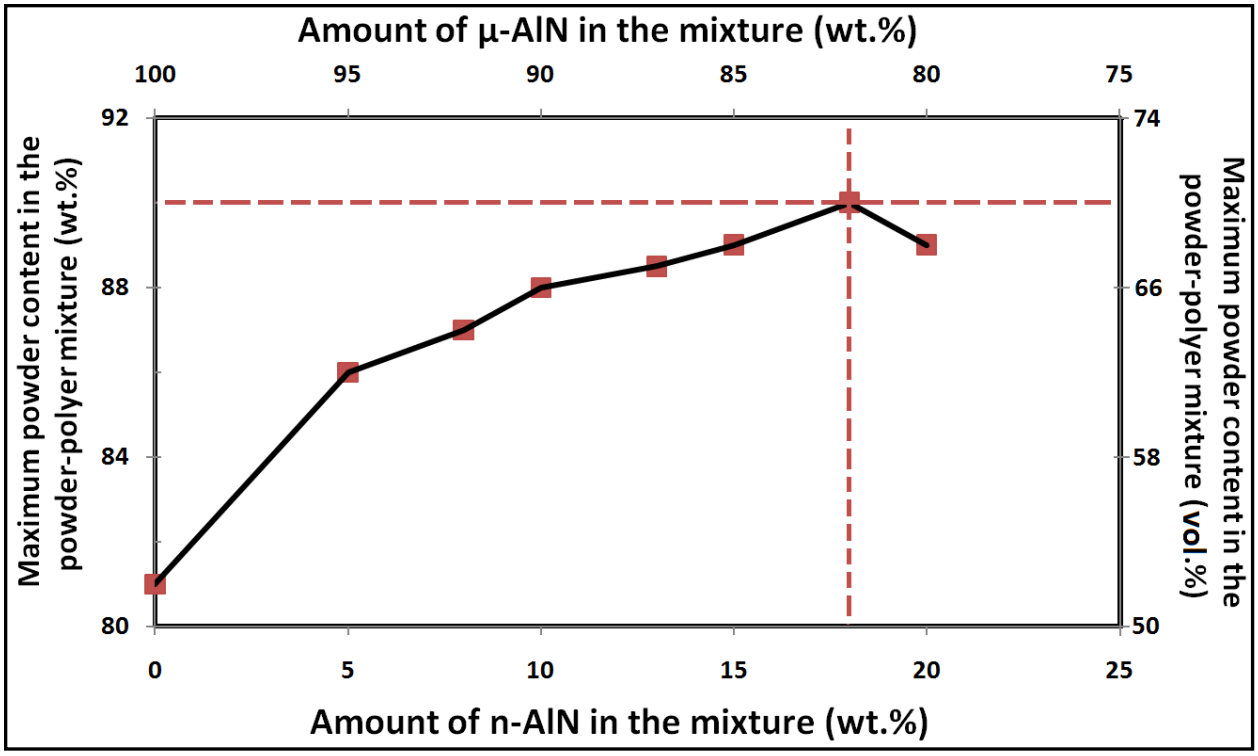

Figure 2a: Effect of n-AlN addition to µ-AlN on the maximum powder fraction in the powder-polymer mixture

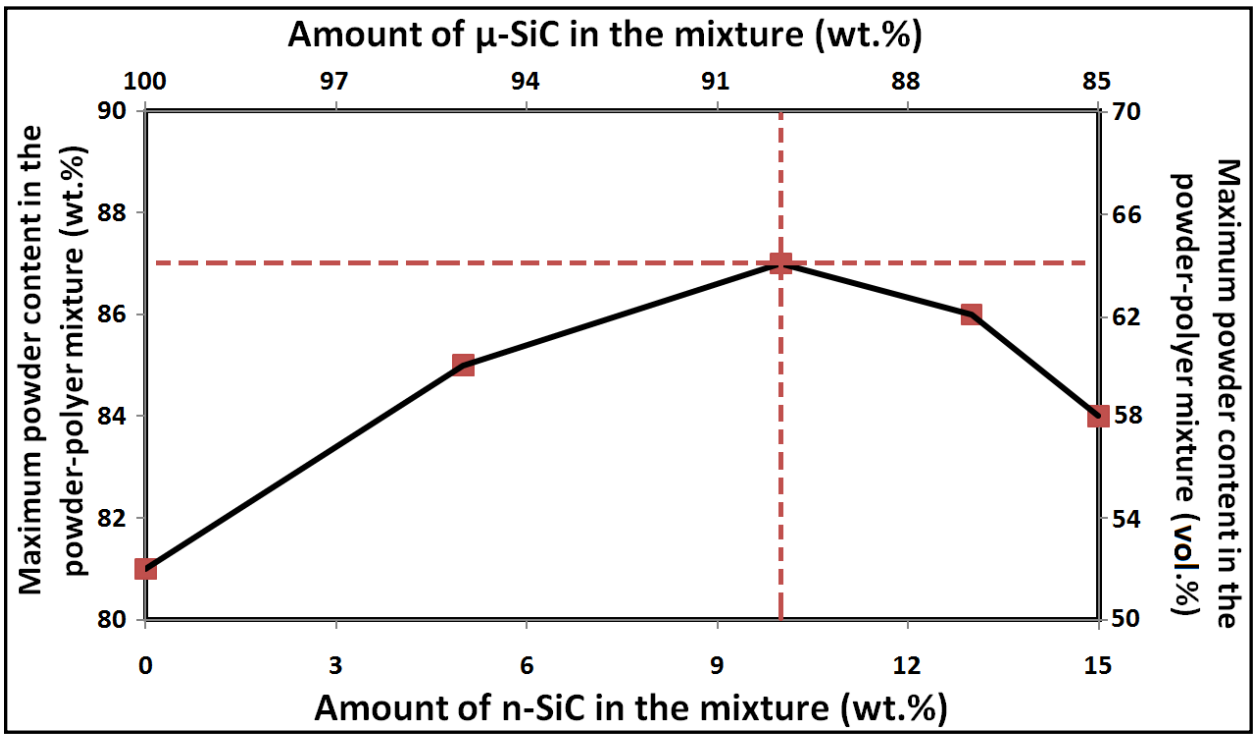

Figure 2b: Effect of n-SiC addition to µ-SiC on the maximum powder fraction in the powder-polymer mixture

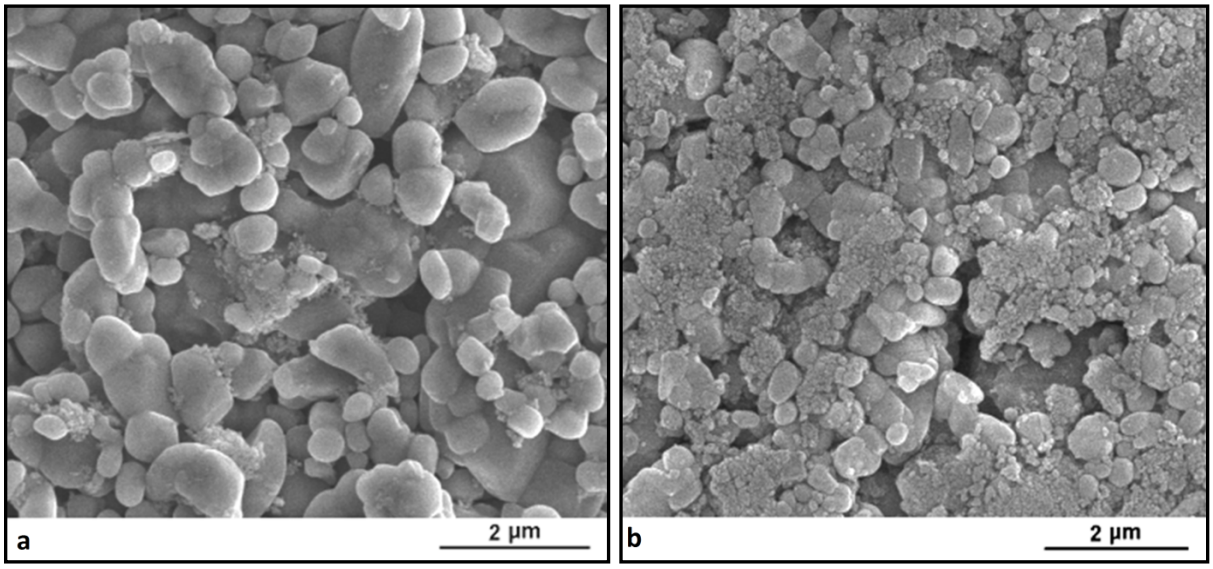

Figure 3: Comparison of powder packing behavior in monomodal (a) and bimodal (b) AlN powder-polymer mixtures

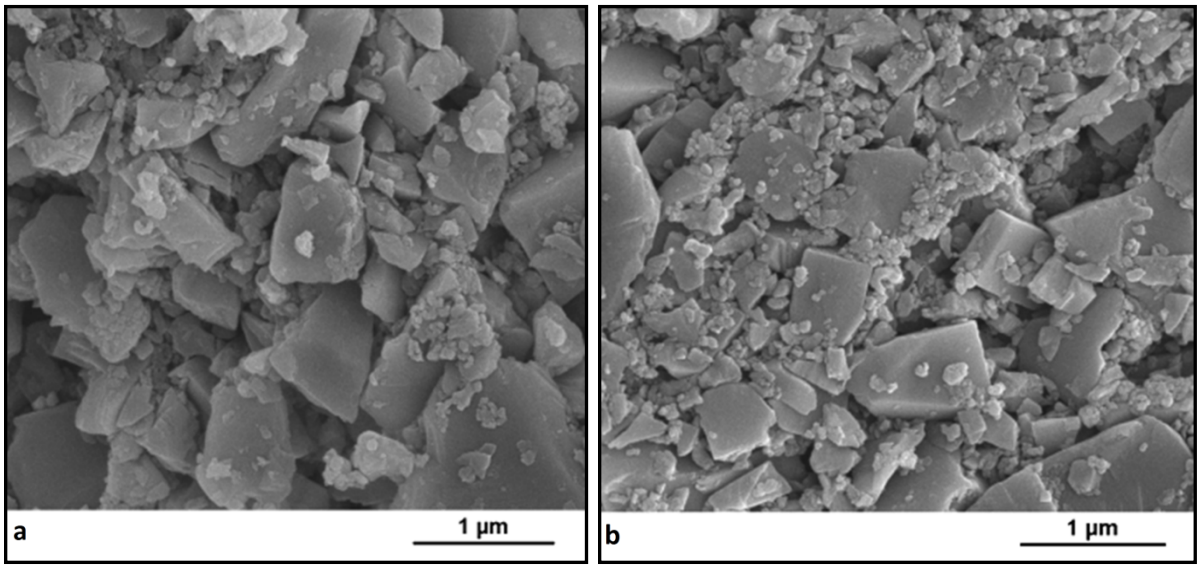

Figure 4: Comparison of powder packing behavior in monomodal (a) and bimodal (b) SiC powder-polymer mixtures

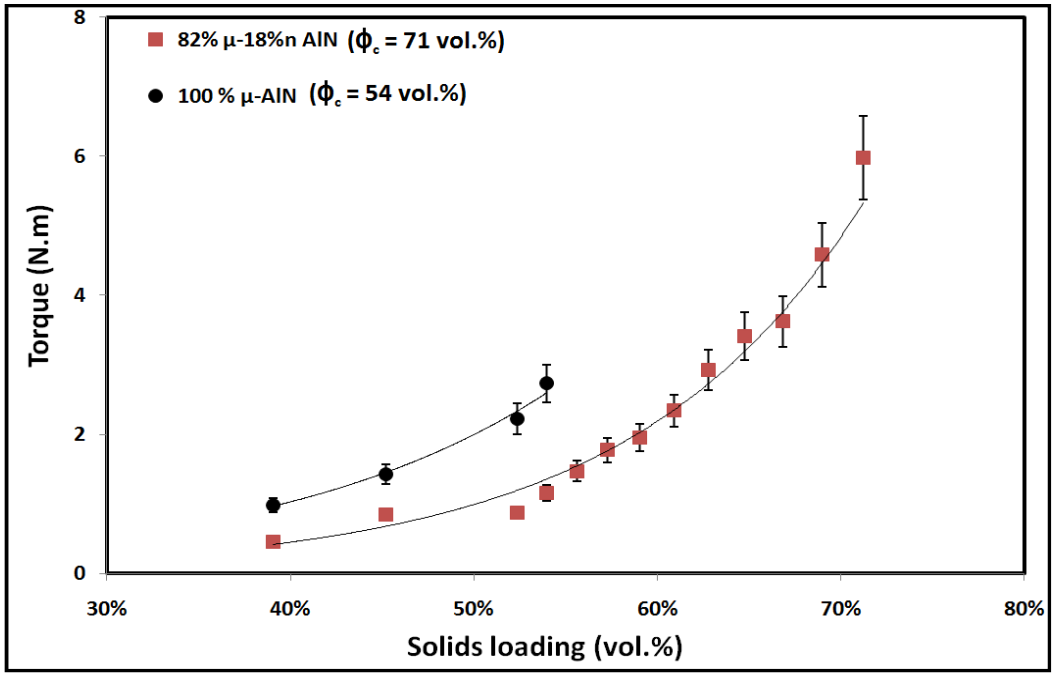

Figure 5a: Effect of nanoparticle addition on the mixing torque of the AlN powder-polymer mixtures

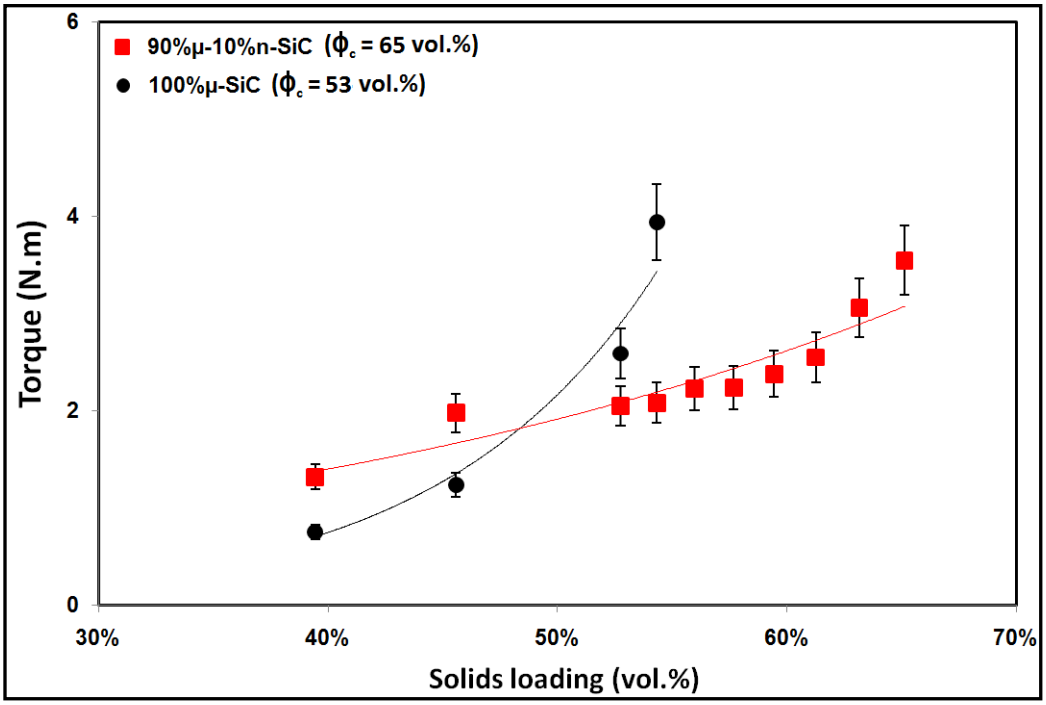

Figure 5b: Effect of nanoparticle addition on the mixing torque of the SiC powder-polymer mixtures

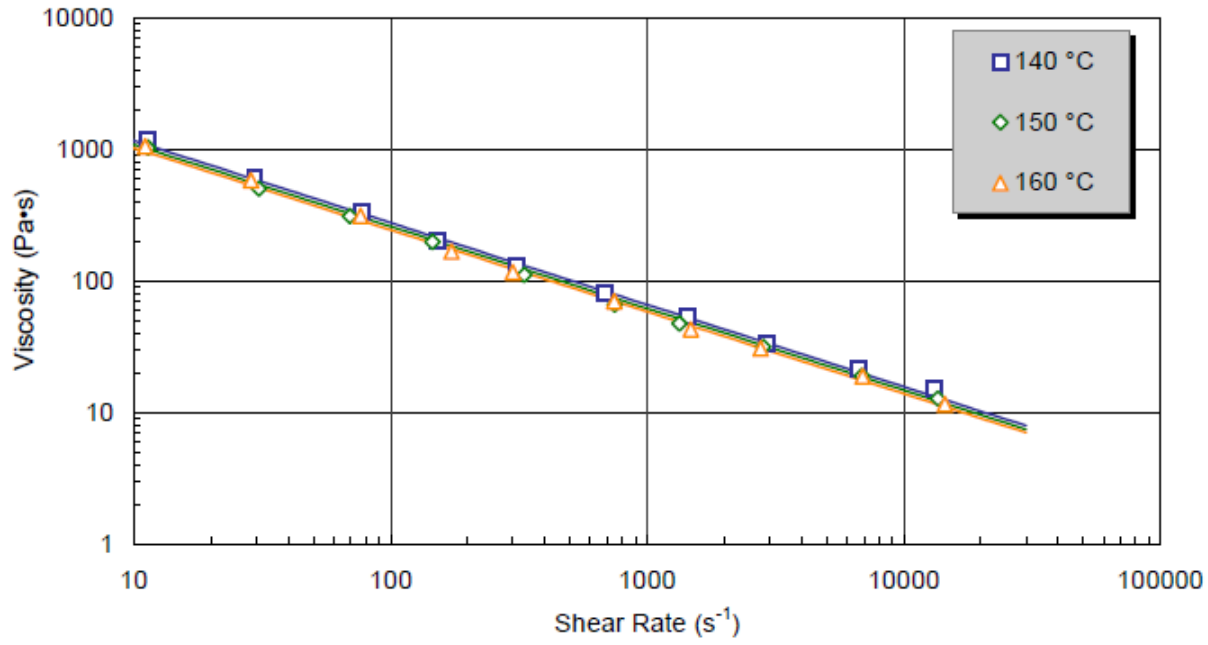

(a)

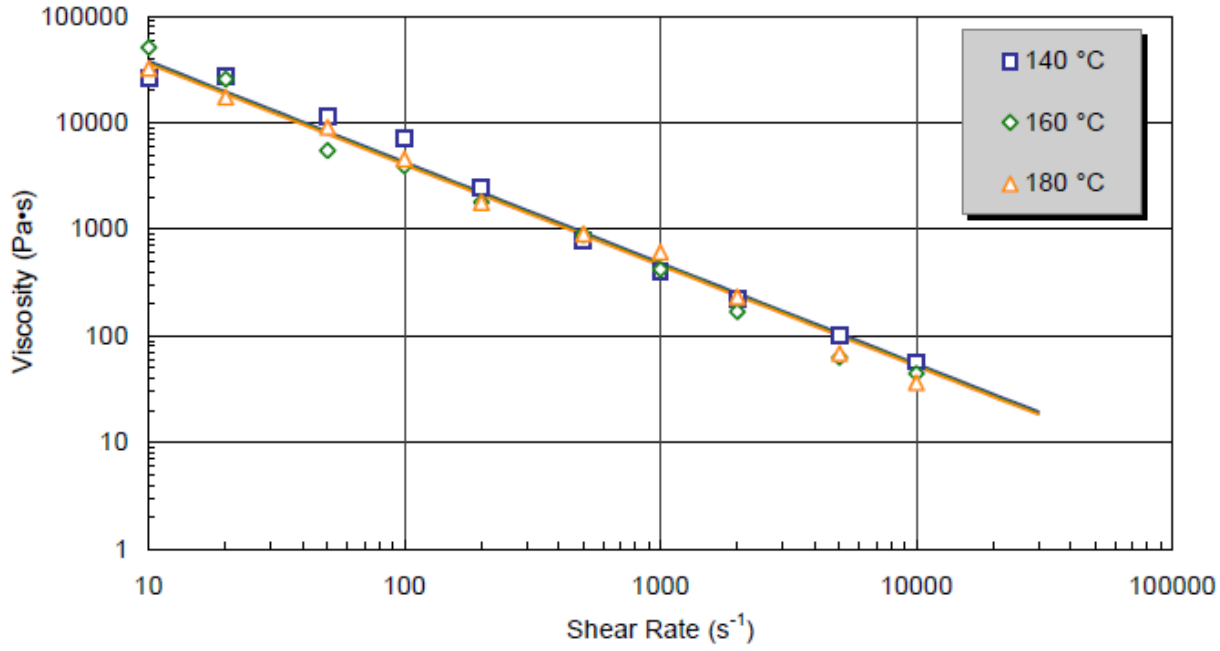

(b)

Figure 6: Viscosity of monomodal (a) and bimodal (b) AlN powder-polymer mixtures at different shear rate and temperature combinations, exhibiting pseudo-plastic behavior

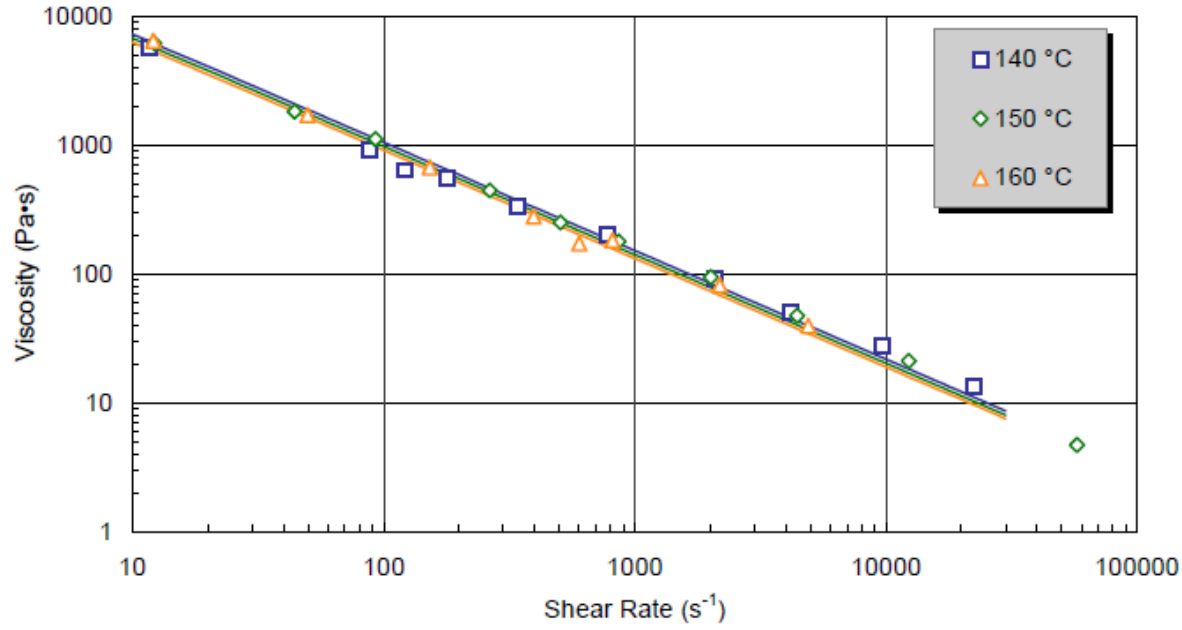

(a)

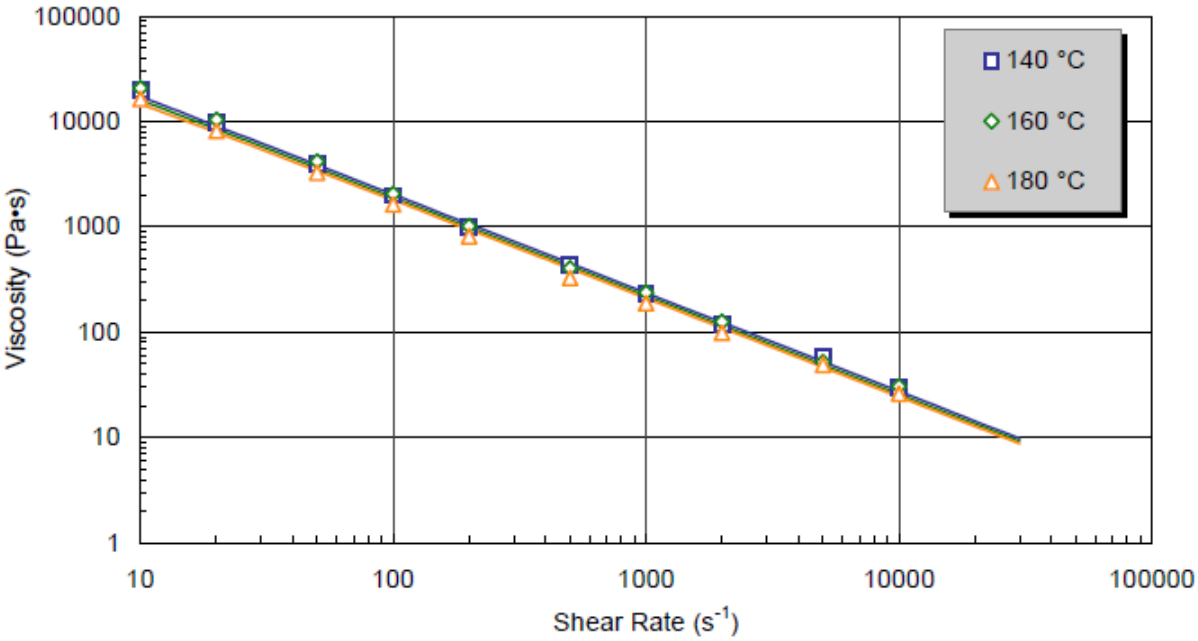

(b)

Figure 7: Viscosity of monomodal (a) and bimodal (b) SiC powder-polymer mixtures at different shear rate and temperature combinations, exhibiting pseudo-plastic behavior

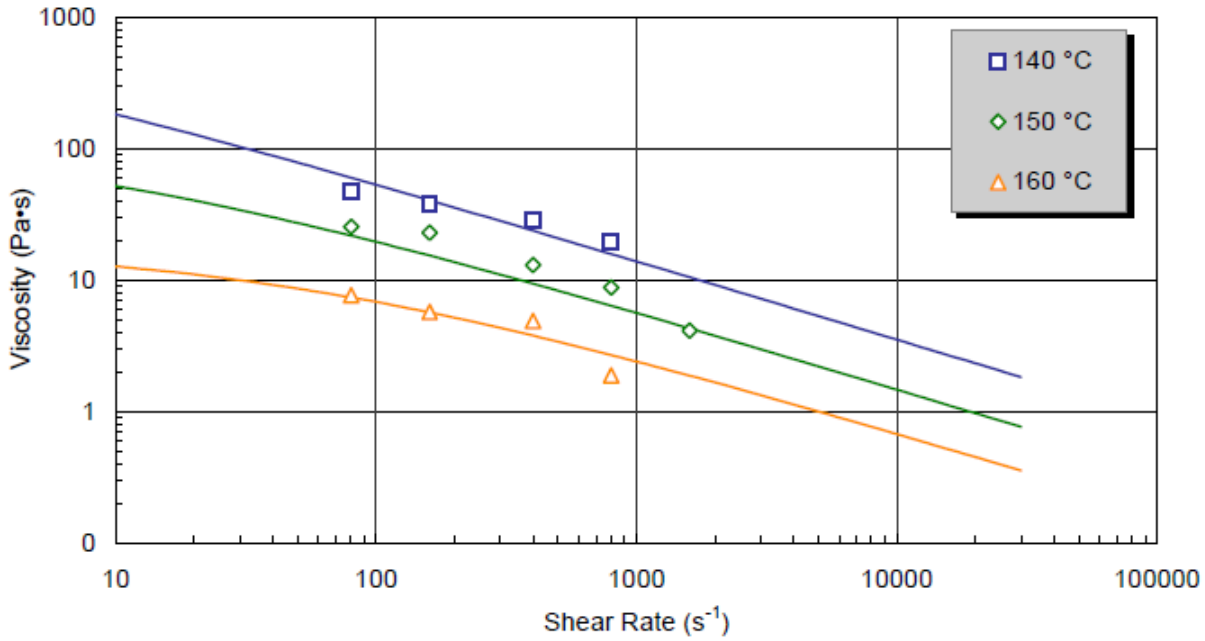

Figure 8: Viscosity of the binder mixture at different shear rate and temperature combinations

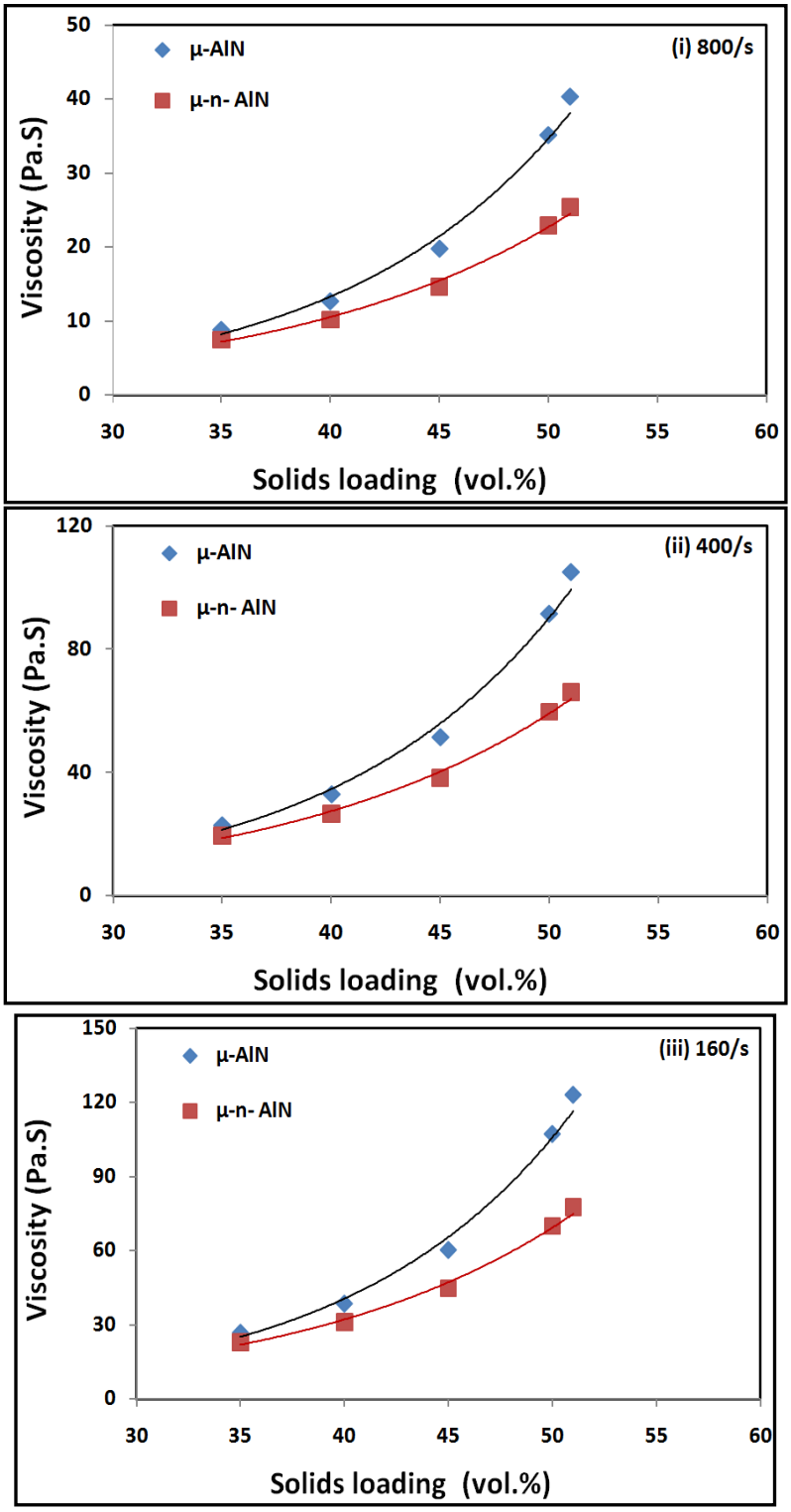

Figure 9a: Comparison of viscosity (calculated by the simplified Krieger-Dougherty model) as a function of solids loading for monomodal and bimodal AlN powder-polymer mixtures at 160 °C for shear rates of (i) 800/s, (ii) 400/s and (iii) 160/s.

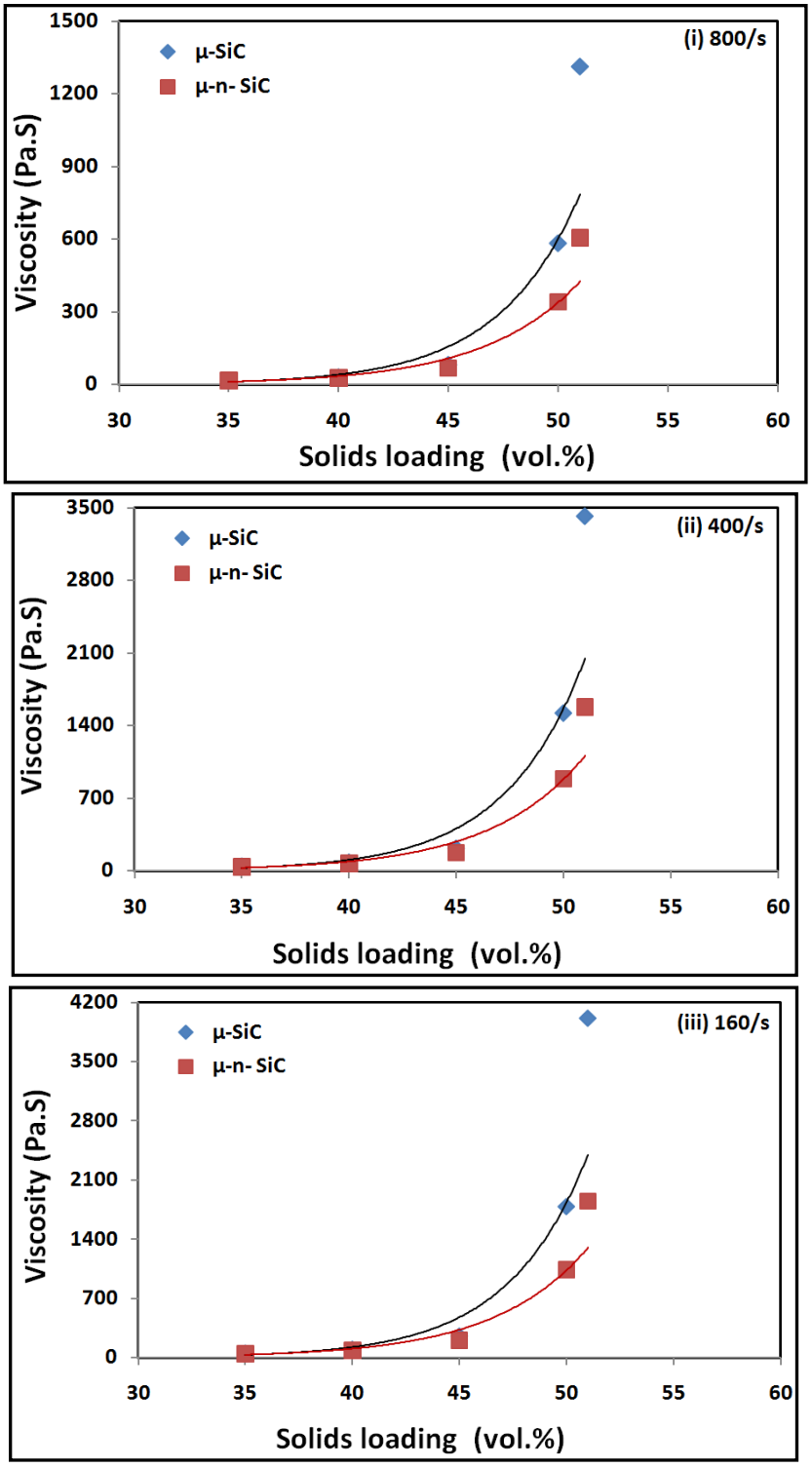

Figure 9b: Comparison of viscosity (calculated by the simplified Krieger-Dougherty model) as a function of solids loading for monomodal and bimodal SiC powder-polymer mixtures at 160 °C for shear rates of (i) 800/s, (ii) 400/s and (iii) 160/s.

.

Table 1: Conditions used for scaling up of SiC and AlN powder-polymer mixtures

Extruder Specifications	Values
Screw Diameter (Co-Rotating)	27 mm
L/D	40
Flight Depth	4.3
Barrels/Zones involved	10
Zone Temperature	160 °C
Screw Speed	260 rpm
Extrusion Rate	30 lb/hr
Cooling System	Air-cooled conveyor belt system

Table 2: Slopes of the viscosity plots of powder-polymer mixtures and binders representing the power law coefficient "n" values

Material	(1-n)	R^2
Binder Mixture	0.61	0.98
Monomodal μ-SiC (51 vol.%)	0.84	0.99
Bimodal μ-n SiC (58 vol.%)	0.93	0.98
Monomodal μ-AlN (52 vol.%)	0.66	1
Bimodal μ-n AlN (65 vol.%)	0.95	0.99